



Enhanced solar cell performance by optimization of spray coated CZTS thin film using Taguchi and response surface method

Siddhant B. Patel¹ · Jignasa V. Gohel¹

Received: 12 October 2017 / Accepted: 4 January 2018 / Published online: 19 January 2018
© Springer Science+Business Media, LLC, part of Springer Nature 2018

Abstract

The present study aims to investigate the optimum deposition conditions for preparation of CZTS thin films using the spray pyrolysis method. CZTS is a vital semiconducting material now days, as it requires the constituents, which are non-toxic and easily available as well. The Taguchi approach is implemented for optimization. Major quality control parameters considered are: copper to zinc plus tin (Cu/Zn + Sn) ratio; zinc to tin (Zn/Sn) ratio; substrate temperature; and spray time. Three levels of each parameter are selected. This attributes L9 (3⁴) orthogonal array according to Taguchi design. The signal to noise (S/N) ratio and an analysis of variance is carried out to achieve an optimum combination of quality control parameters. In the present study, thin films are optimized in terms of the band gap. The solar cell is fabricated for each experiment and for an optimum combination as well. A novel cell fabrication (inverted) is introduced which can cover full light spectra. The cell is fabricated as FTO/i-ZnO/Al:ZnO/CdS/CZTS/CuS/FTO. More than 17% improvement in efficiency is observed by the cell fabricated using optimum condition than the best efficiency achieved by orthogonal array 2, among all 9 arrays. Furthermore, to achieve specific optimum condition, response surface methodology (RSM) is implemented. The RSM is carried out for a multiple response (band gap and efficiency). The films are characterized by X-ray diffraction and field emission scanning electron microscopy. Optical properties are studied by UV–Visible spectroscopy. The elemental study is carried out using energy-dispersive X-ray spectroscopy.

1 Introduction

The kesterite materials based thin film solar cells are drawing considerable attention attributed to its excellent environmental stability and low-cost [1]. At present, copper indium gallium selenide (CIGS) and cadmium telluride (CdTe) absorber material based solar cells are available commercially in the market. These materials based solar cells have achieved more than 20% efficiency on the laboratory scale [2]. However, due to the toxicity issue of cadmium and gallium, and less availability of indium and telluride, the large scale production is limited [3]. CZTS is emerging as a promising alternative absorber material, attributed to less

toxicity and easily available constituents [4]. Furthermore, it has a direct band gap of 1.4–1.6 eV and high absorption coefficient (10⁴ cm⁻¹) with p-type conductivity [5]. So far, 12.7% efficiency is reported for the CZTS based solar cells in recent years [6], which is quite encouraging. However, it is still less than theoretically calculated by Shockley and Queisser (32%) [7].

Up till now, various techniques are reported to develop CZTS thin films, such as sputtering [8], electro-deposition [9], thermal evaporation [10], pulse laser deposition [11], chemical vapor deposition [12], sol–gel spin coating [13], spray pyrolysis [14], etc. To reduce the further cost of solar cell preparation, the chemical based technique can be employed [15, 16]. Among these techniques, spray pyrolysis is considered as the most appropriate technique for the preparation of low-cost thin film solar cells [17]. This technique can be easily employed for the large-scale production as well. Till now, numerous researchers have reported preparation of CZTS thin films using spray pyrolysis method [18–23]. The physical properties of CZTS thin films are utterly dependent on the process parameters and condition. If the process conditions are not appropriate, a secondary

Electronic supplementary material The online version of this article (<https://doi.org/10.1007/s10854-018-8530-5>) contains supplementary material, which is available to authorized users.

✉ Jignasa V. Gohel
jignasa.narsinhbhai@gmail.com; sjn@ched.svnit.ac.in

¹ Department of Chemical Engineering, Sardar Vallabhbhai National Institute of Technology, Surat, Gujarat 395 007, India

or ternary phase occurrence may take place [24]. Thus, it is essential to determine values of the major thin film quality control parameters (with best combination) to obtain the optimum thin film for solar cell applications. All the quality control parameters are listed in our previous review paper [25]. The maximum studies on optimization have considered one factor at a time for the CZTS thin film optimization. The effect of substrate temperature on CZTS thin film properties is reported in the literature [26–28]. The effect of copper content on CZTS thin film properties is well reported [29–31]. The higher Zn/Sn ratio leads to enhanced CZTS film properties [22, 32, 33]. Rajeshmon et al. [34] studied the effect of spray rate on the properties of CZTS film. However, to the best of Author's knowledge, a comprehensive study on the simultaneous effect of each of the major parameters for optimization of spray coated CZTS thin film is not yet reported.

To carry out this kind of comprehensive study, design of experiments (DoE) method can be implemented. The most efficient DoE method reported are factorial design, Taguchi method, response surface methodology, contour mapping, grey analysis, etc [35]. When a single response optimization based on multiple parameters is area of interest then, Taguchi method is superior DoE method as less number of experiments is required to identify the optimum condition. If four parameters are varied at three different levels, 81 experiments are required to identify the optimum combination. Whereas, Taguchi method uses the orthogonal array design and the analysis of variance (ANOVA) to identify the interaction of the control parameters with the response, hence it can give optimum combination in only 9 experiments [36]. However, Taguchi method will give an optimum combination of the controlling parameters. If a specific optimum condition or multi-response optimization based on multiple parameters is area of interest then, response surface methodology (RSM) is the superior method. RSM method generates a mathematical model between the parameters and desired responses based on experimental design [37]. Two types of designs, namely, Central Composite design (CCD) and Box–Behnken design (BBD) are used in RSM. These designs requires more number of experiments than Taguchi (31 in CCD and 29 in BBD), still these are less than conventional (81). Finally, mathematical model is optimized and specific optimum condition can be achieved.

In the present study, the spray pyrolysis method is employed for the CZTS thin film preparation. The four essential thin film quality control parameters, namely, Cu/Zn + Sn ratio, Zn/Sn ratio, substrate temperature and spray time, are studied in detail. Furthermore, to obtain the optimum combination of control parameters the Taguchi approach with L9 orthogonal array design is used. The effect of parameters on optical, structural and surface properties of the thin film are studied using UV–Visible, X-ray diffraction

(XRD) and field emission scanning electron microscopy (FE-SEM), respectively. Furthermore, the solar cells are fabricated for all 9 thin films prepared using L9 orthogonal array as well as optimum condition successfully. A novel cell fabrication (inverted) is proposed based on tandem cell principle. The cell is fabricated as FTO/i-ZnO/Al:ZnO/CdS/CZTS/CuS/FTO. Additionally, to obtain optimum process condition with multiple responses, the RSM is carried out.

2 Experimental

2.1 Materials

Copper (II) chloride ($\text{CuCl}_2 \cdot 2\text{H}_2\text{O}$), zinc acetate [$\text{Zn}(\text{O}_2\text{CCH}_3)_2(\text{H}_2\text{O})_2$], tin chloride ($\text{SnCl}_2 \cdot 2\text{H}_2\text{O}$), thiourea [$\text{SC}(\text{NH}_2)_2$], cadmium acetate [$\text{Cd}(\text{OCOCH}_3)_2$] and isopropyl alcohol (IPA) of analytical grade were purchased from S. D. Fine chemicals, India. A fluorine doped tin oxide (FTO) glass substrate was purchased from Sigma-Aldrich. Argon gas was used for annealing. All the chemicals were used without further purification.

2.2 Methodology

2.2.1 CZTS thin film preparation by spray pyrolysis

The spray pyrolysis method was implemented to prepare CZTS films on the FTO glass substrate. The precursor solution was prepared by dissolving 0.1 M precursor of Cu, Zn, Sn and S into a mixture of IPA and water (2:1). Few drops of monoethanolamine were added as a stabilizer. Thiourea was provided in excess (three times) than its stoichiometric requirement to compensate the sulfur loss during spray pyrolysis. The precursor solution was sprayed for the specific time on the heated glass substrate. Air was used as carrier gas and its pressure was kept constant (2 bar) throughout all the experiments. The distance between nozzle and substrate was kept constant (20 cm). The molar concentration of precursors (Cu, Zn and Sn), substrate temperature and spraying time were varied at three levels as shown in the Table 1. Then the film was annealed at 500 °C under an argon atmosphere to avoid sulfur annealing, which is a toxic approach

Table 1 CZTS thin film quality control parameters and their levels in the thin film preparation

Parameters	Level 1	Level 2	Level 3
Cu/Zn + Sn (A)	0.8	1	1.2
Zn/Sn (B)	0.9	1	1.1
Sub Temp (°C) (C)	280	320	360
Spray Time (S) (D)	5	10	15

of annealing. The CZTS films were prepared according to Taguchi design L9 array as shown in Table 2. Nine experiments are termed as R1–R9.

2.2.2 Taguchi method

Taguchi method utilizes distinct design of orthogonal array to study the entire range of parameters with a very less number of experiments. For the selection of appropriate orthogonal array, the essentials are (i) enlist the process parameters and interactions to be assessed (ii) the number of levels (variation) for the selected parameters, and (iii) the estimation of the total degree of freedom based on the number of parameters as well as their levels. The analysis of experimental data and the optimum combination of process parameter is determined using signal-to-noise ratio (S/N). The influence of the process parameters on the response (result) is determined by ANOVA. At the end of completion of the procedure, a combination of control parameters is acquired, which may lead to the optimum results. In the present study, four factors (quality control parameters) were enlisted, namely, copper to zinc + tin ratio (Cu/Zn + Sn) (A), zinc to tin ratio (Zn/Sn) (B), substrate temperature (C) and spray time (D). More than two levels of the parameters must be examined to understand the non-linear behavior of the process parameters (if exists). Hence, the parameters were varied at 3 level, which implies L9 (3⁴) orthogonal array. The band gap of CZTS is considered as the response of experiments. The objective of the study is to minimize the band gap of CZTS to the optimum reported band gap (1.5 eV). Hence, the smaller-is-better was preferred for the estimation of S/N ratio. The S/N ratio was calculated using the following equation:

$$\frac{S}{N_i} = -10 \log \left[\frac{1}{n} \sum_{j=1}^n Y_{ij}^2 \right] \tag{1}$$

where, i is an experiment, n is number of experiment carried out, Y_{ij} is the measured value for i and j = 1 to n. Table 2

illustrates the orthogonal array of the 9 thin film preparation conditions used for calculating the signal to noise ratio (S/N ratio). Each experiment was carried out two times and an average of two values was used for S/N ratio calculation. All the analysis and calculation in this present study were carried out using Microsoft Excel.

2.2.3 Response surface methodology

Although Taguchi approach has the benefit of few experiments, it has a limitation as well. Taguchi approach is not applicable for the multiple response optimization. The traditional method for multiple response optimization is overlaid the contour plots. However, it is beneficial up to two or three parameters only; if more than three parameters are introduced then it loses its efficiency. Hence, other optimization methods such as, grey analysis, factorial design, RSM, etc. are introduced, in which RSM is more preferable as it gives a specific optimum value from entire range for each parameter using mathematical models. Initially, Box and Draper had introduced the RSM for modeling the experimental responses in 1987 [38]. Later on, it is used as an optimization tool. The RSM became more common after Venter et al. [39] discussed advantages of RSM in the optimization. RSM creates a mathematical model for specific problem based on designs of experiments and hence, it gives a specific optimum condition. Typically, two types of experimental designs namely, (i) Central composite and (ii) Box–Behnken are available. The Central composite design follows the full quadratic model, whereas Box–Behnken can be applied to first and second order models. Box–Behnken requires three levels per parameters. Hence, the same parameter and their levels used in Taguchi approach are considered for RSM. According to the Box–Behnken design of experiments, four factors and three levels and five central point leads to the 29 experiments. All the analysis and calculation, as well as optimization were carried out using Design Expert V10.

Table 2 L9 Orthogonal array along with EDX results

No.	Factors				EDX results		Band gap		S/N ratio
	A	B	C	D	Cu/Zn+ Sn	Zn/Sn	B1	B1	
R1	0.8	0.9	280	5	0.82	0.93	1.86	1.91	−5.507
R2	0.8	1	320	10	0.86	0.97	1.53	1.55	−3.765
R3	0.8	1.1	360	15	0.83	1.08	1.66	1.61	−4.271
R4	1	0.9	320	15	1.01	0.88	1.70	1.71	−4.635
R5	1	1	360	5	1.00	1.02	1.81	1.79	−5.106
R6	1	1.1	280	10	1.04	1.14	1.73	1.75	−4.811
R7	1.2	0.9	360	10	1.17	0.92	1.85	1.83	−5.296
R8	1.2	1	280	15	1.18	1.00	1.98	2.05	−6.087
R9	1.2	1.1	320	5	1.19	1.08	1.60	1.63	−4.164

2.2.4 Device fabrication

Firstly, the FTO substrate (20 mm × 20 mm × 2 mm) was etched with Zn powder and 2 M HCl diluted in water, and then cleaned with DI water, followed by sonication with acetone (10 min). Further, it was rinsed in double distilled water and lastly dried under vacuum oven at 60 °C. In frequently reported CZTS cell structure, the electron transport layer (ETL) (ZnO and CdS) is coated on the top of CZTS layer. In this study, the cell fabrication is inverted. The ETL layers were deposited upon the transparent electrode (FTO) and hole transport materials (HTM) were coated on the top of ETL in order to utilize light spectra in large amount. In our previous work, we have optimized the ZnO layer [40]. In the present study, the same procedure was followed to prepare ZnO layer. A clear solution of ZnO was prepared by dissolving zinc acetate in IPA + water mixture (2:1) and sprayed on the heated (365 °C) FTO substrate. Previously we have reported application of Cu and Ag doped ZnO layer [41, 42]. In present study, Al-doped ZnO solution was prepared and sprayed on the ZnO layer at the same substrate temperature. Further, the CdS layer was deposited by spraying a clear aqueous solution having 0.1 M of cadmium acetate and 0.1 M of thiourea (at 320 °C substrate temperature). Consequently, the CZTS solution was deposited on the CdS layer.

The CuS/FTO was used as the counter electrode. The CuS solution was prepared by dissolving 0.1 M copper chloride and 0.1 M thiourea in IPA-water mixture (2:1). It was sprayed at 320 °C substrate temperature. To study the statistics of solar cell performance, five solar cells were fabricated for each array as well as for optimum combination thin film based solar cell. Further, forward and reverse scanning was carried out for optimum thin film based solar cell.

2.2.5 Characterization

The band gap of CZTS film was evaluated by the Tauc's plot using UV-Vis (HACH-DR 6000/2 UV spectrometer) within the range of 300–1100 nm at room temperature. The structural properties of thin films and the consequent solar cells were analyzed by XRD (Rigaku D/Max 2200). Cu-K α_1 was used as the source of the X-rays with the wavelength of 1.5418 Å. The surface morphology of the thin film was studied using a field emission scanning electron microscope (FE-SEM, Joel JSM-7600F, JEOL Ltd.) and the elemental composition study of CZTS film was carried out using the scanning electron microscopy (SEM, S3400, Hitachi International Ltd.) accompanied with energy dispersive X-ray spectroscopy (EDX). The SEM images were taken under high vacuum (10⁻⁵ bar). The EDX data were measured at three different locations for each of the sample. The J-V characteristic of the solar cell was recorded using Keithley 2400 solar simulator (Keithley Instruments, Inc, USA) under

Table 3 Factor response table of S/N ratio

Level	A	B	C	D
1	-4.51	-5.15	-5.47	-4.93
2	-4.85	-4.99	-4.19	-4.62
3	-5.18	-4.42	-4.89	-5.00

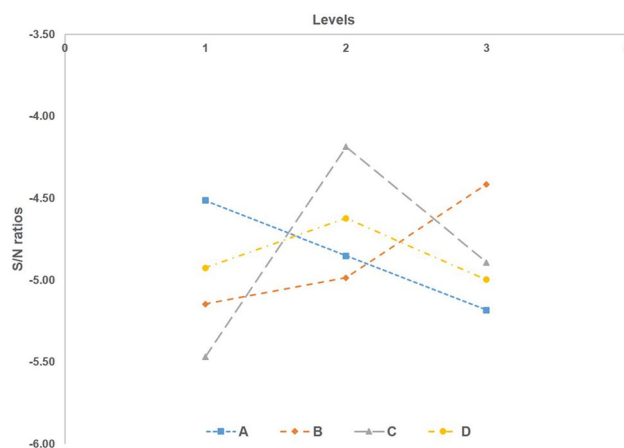


Fig. 1 The means of signal-to-noise for smaller is better

AM 1.5G illumination at 100 mW cm⁻². A xenon lamp was used as a source of light.

3 Result and discussion

3.1 Analysis of signal-to-noise ratio and variance

Table 2 depicts the experimental data of the band gap and corresponding S/N ratios. The elemental analysis of all the samples (R1–R9) is also shown in Table 2 (See the results of EDX results in Supporting Info). The mean S/N ratio for each of the control parameter is calculated based on Table 2. The mean S/N ratio of each of the control parameter at each level is listed in Table 3. Figure 1 depicts the value of mean S/N ratios graphically. The greater value of S/N ratio indicates that the band gap is low. As observed from Table 3, the optimum combination is A₁ = 0.8 (Cu/Zn + Sn), B₃ = 1.1 (Zn/Sn), C₂ = 320 °C (substrate temperature) and D₂ = 10 s (spray time). The ANOVA is performed to determine the significance (contribution) of quality control parameters on the response (the band gap). The results of ANOVA for the band gap are listed in Table 4. The substrate temperature demonstrated a prominent effect on the band gap, as its contribution is largest (57.97%). The second most affecting parameter is the Zn/Sn ratio (20.77%) and third contributing parameter is the Cu/Zn + Sn ratio (15.72%). However, spray

Table 4 ANOVA results of Taguchi Method

Factors	Sum of squares	Degree of freedom	Variance	F-test	Contribution P (%)
A	0.07	2.00	0.037	2.84	15.72
B	0.10	2.00	0.049	3.75	20.77
C	0.27	2.00	0.137	10.48	57.97
D	0.03	2.00	0.013	1.00	5.53
Error	0.00	0.00			
Total	0.47	8.00			
Pooled error	0.03	2.00	0.013		

time contributed lowest effect on band gap (5.53%). Hence, it is considered insignificant.

3.2 Optical analysis of orthogonal array

The band gap of each of the sample is estimated from the Tauc’s plot using following equation:

$$(\alpha h\nu)^2 = h\nu - E_g$$

where, α is the absorbance coefficient and $h\nu$ is photon energy. The band gap of all the samples is observed to be varying from 1.53 to 1.98 eV (see Fig. 2). It is observed that at low substrate temperature (280 °C) the band gap is higher than desired band gap value for CZTS film [43–47]. However, increase in temperature led to reduction in the band gap. Hence, the substrate temperature is observed to be the prominent control parameter, which is in agreement with ANOVA results (Table 4).

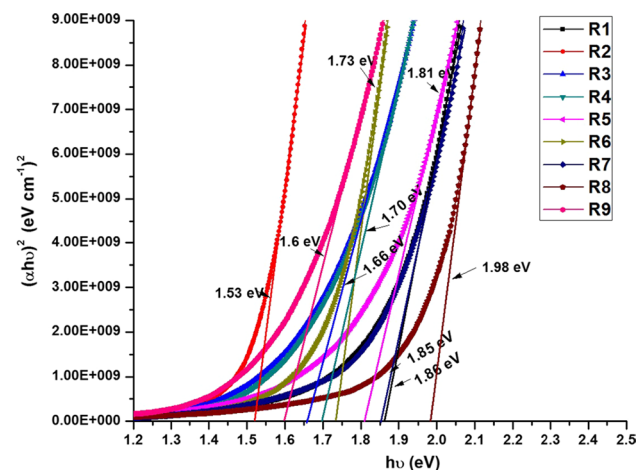


Fig. 2 $(\alpha h\nu)^2$ versus $(h\nu)$ plot of all the nine samples of CZTS thin films

3.3 Structural analysis of orthogonal array

The presence of secondary phase in CZTS thin film may attribute to the enhanced band gap. Numerous authors have reported the presence of secondary phase, copper based (CuS, Cu_xS , etc.) for Cu-rich film [48–51] and zinc based (ZnS, $ZnSnS_3$, etc.) in Zn-rich film [52, 53]. The XRD analysis of the as-deposited film is carried out for all the experiments and the results are illustrated in Fig. 3. Daranfied et al. [52] has reported that the secondary phase formation also depends on the type of solvent. Use of water as a type of solvent may lead to copper based secondary phase, whereas alcohol as solvent may lead to zinc based secondary phase. In the present study, both copper-based (CuS and Cu_2S) and zinc-based (ZnS and $ZnSnO_3$) secondary phases are obtained. This result may be attributed to the presence of both IPA and water.

The XRD peaks are observed at 2θ values of 28.5°, 32.8°, 46°, 56.52° and 69°, corresponding to (112), (200), (220), (312) and (008) planes respectively. The results are in good agreement with generally reported CZTS kesterite structure in the literature [54–57]. In addition, in all the samples, a secondary phase of ZnS is also observed. However, at optimum temperature (320 °C), the impurity of ZnS is negligible (as observed in Fig. 3, from lesser intensity corresponding to ZnS). The impurity of ZnS is present at low temperature (280 °C), however, attributed to large band gap value. Similarly, at high temperature (360 °C) also, minor impurity of ZnS is present. In addition, $ZnSnO_3$ is also present due to oxidization.

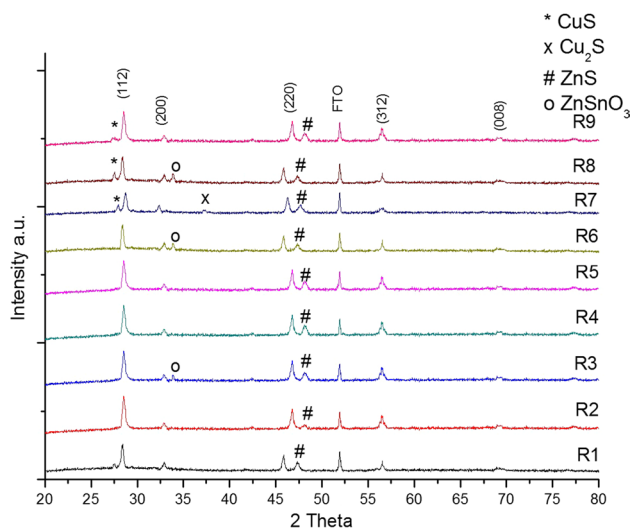


Fig. 3 XRD analysis of all the nine samples of CZTS thin films

3.4 Morphological analysis of orthogonal array

Figure 4 depicts the surface morphology of all the samples. Larger grains (agglomerated) and non-uniform films are obtained at low temperature (280 °C, represented as R1, R6 and R8). Upon increment in temperature from 320 (see R2, R4 and R9) to 360 °C (see R3, R5 and R7), the grain size is reduced and uniformity is increased. Although spray time is not highly affecting parameter for band gap, it affects surface morphology to some extent. The low spray time (5 s) led to voids in morphology (R1, R5 and R9). In addition, high spray time (15 s) also led to undesired agglomeration (R3, R4 and R8). A uniform and dense morphology is observed at optimum spray time (10 s). The superior result is achieved at R2.

3.5 Solar cell characterization of orthogonal array

The solar cells fabricated with all the samples are further characterized by solar simulator. The solar cell efficiency is measured under AM 1.5G illumination at 100 mW cm^{-2} .

The statistics of all nine solar cells and J–V characteristics for all the nine samples are shown in Fig. 5 and Table 5,

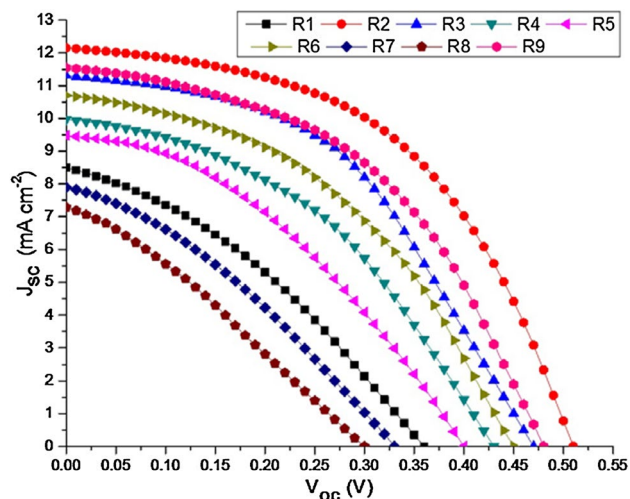


Fig. 5 J–V characteristics of all the solar cells

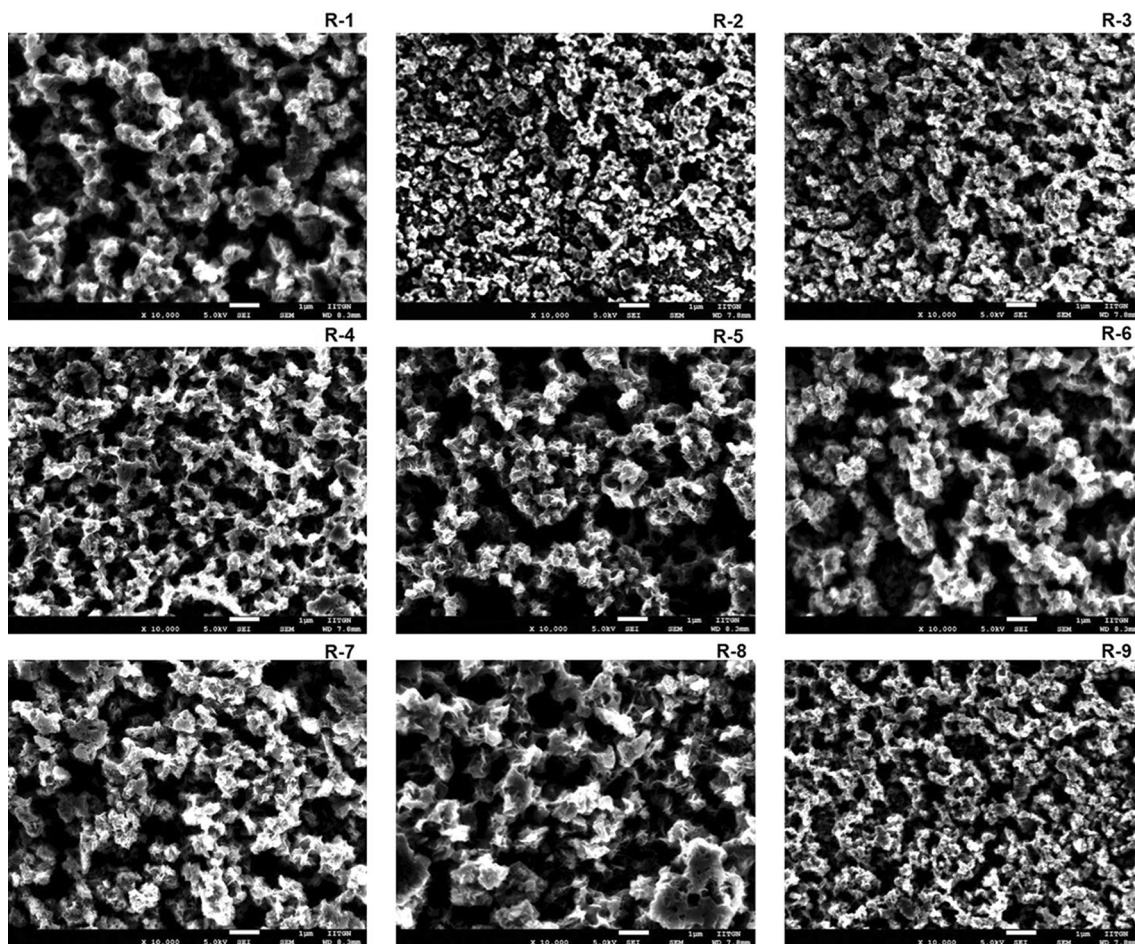


Fig. 4 Surface morphology of all the nine samples of CZTS thin films

Table 5 Statistics of solar cell of all nine solar cells

No.	J_{SC} (mA cm ⁻²)	V_{OC} (mV)	Fill factor (%)	Efficiency (%)
R1	8.5 ± 0.50	360 ± 7.6	35.0 ± 1.58	1.07 ± 0.14
R2	12.15 ± 0.35	510 ± 4.9	50.0 ± 1.00	3.10 ± 0.18
R3	11.3 ± 0.30	470 ± 5.2	46.5 ± 0.70	2.47 ± 0.13
R4	9.97 ± 0.59	430 ± 9.1	42.0 ± 1.89	1.80 ± 0.24
R5	9.48 ± 0.56	400 ± 8.5	38.5 ± 1.74	1.46 ± 0.19
R6	10.7 ± 0.63	450 ± 9.5	43.0 ± 1.94	2.07 ± 0.27
R7	7.9 ± 0.47	330 ± 7.0	33.0 ± 1.49	0.86 ± 0.11
R8	7.29 ± 0.43	300 ± 6.4	29.5 ± 1.33	0.65 ± 0.08
R9	11.54 ± 0.68	480 ± 10.2	47.0 ± 2.12	2.60 ± 0.32

respectively (see extensive information containing table in Supporting Info as Table 1). Basically, the solar cell efficiency is dependent on band gap and morphology. Additionally, copper percentage (Cu/Zn + Sn ratio) also can affect efficiency. If this ratio is less, efficiency can be high. Fundamentally, copper reduces the shunt resistance and which leads to poor cell performance as reported in various literatures [14, 28, 33, 34, 55]. The superior efficiency and small variation is achieved with the combination of control parameters suggested in R2. The solar cell exhibited 3.10 ± 0.18% of power conversion efficiency (PCE) with V_{oc} , J_{sc} , and FF of 510 ± 4.9 mV, 12.15 ± 0.35 mA cm⁻² and 50 ± 1.00%, respectively. (See cross section and XRD of full solar cell in Supporting Info as Fig. 1 and 2, respectively).

3.6 Confirmation test

In the present study, Taguchi optimization (L9) is performed successfully. Best result among all the 9 orthogonal arrays is achieved with R2 array. The optimum design parameters selected are Cu/Zn + Sn 0.8; Zn/Sn 1.1; substrate temperature 320 °C; and spray time 10 s. The quality characteristic enhancement using the optimum combination (of design parameter) is consequently verified at the final step. Further, a comparison of result of optimum combination with the

results of R2 is also done, to check whether any enhancement is achieved or not. Table 6 depicts the result of comparison between R2 as well as optimum combination. It clearly indicates that the results achieved by the optimum combination are superior to the results achieved by R2. Figure 6 depicts the Tauc's plot, XRD analysis and the SEM image of the film prepared using optimum combination. It also depicts the J–V characteristics of forward scan as well as reverse scan of solar cell prepared using optimum combination. The band gap achieved with optimum combination is favorably less (1.49 eV) than that achieved with R2 (1.53 eV). Additionally, the peak intensity of (112) plane with optimum combination is also favorably higher than that with R2. Not only that, the morphology is also good (dense and uniform). In particular, more than 15% improvement in efficiency and decrement in variation is observed for the solar cell prepared using optimum combination (3.63 ± 0.10%) than that with R2 (3.10 ± 0.18%). The fill factor is also improved from 50 ± 1.00 to 53 ± 0.50%. Further, the optimum combination based solar cell demonstrated negligible hysteresis effect as 3.56 ± 0.14% efficiency is achieved in reverse scan.

3.7 Response surface methodology

Table 7 illustrates the Box–Behnken experimental design along with both responses (band gap and efficiency). The analysis is carried out in Design Expert V10. The full quadratic model is selected while analyzing RSM. Table 8 depicts the ANOVA results obtained. With multiple responses, the substrate temperature is yet again observed to be the prominent control parameter (p-value < 0.05 in both response). R² values observed are also nearly unity for the band gap model (99.69%) and efficiency model (99.70%). Hence, it is clear that the suggested model is highly valid.

Further, using the 'Optimization' feature of software, the optimum condition is obtained. The optimum condition obtained is A = 0.8 (Cu/Zn + Sn ratio), B = 1.1 (Zn/Sn ratio), C = 327.34 °C (≈ 330 °C) (substrate temperature)

Table 6 Comparison between the results of R2 and optimum combination based on Taguchi optimization

	R2	Optimum based on Taguchi (forward scan)	Optimum based on Taguchi (reverse scan)
Band gap (eV)	1.53	1.49	1.49
J_{SC} (mA cm ⁻²)	12.15 ± 0.35	12.67 ± 0.20	12.80 ± 0.25
V_{OC} (mV)	510 ± 4.9	540 ± 2.2	530 ± 3.9
Fill factor (%)	50.0 ± 1.00	53.0 ± 0.50	52.5 ± 0.60
Efficiency (%)	3.10 ± 0.18	3.63 ± 0.10	3.56 ± 0.14

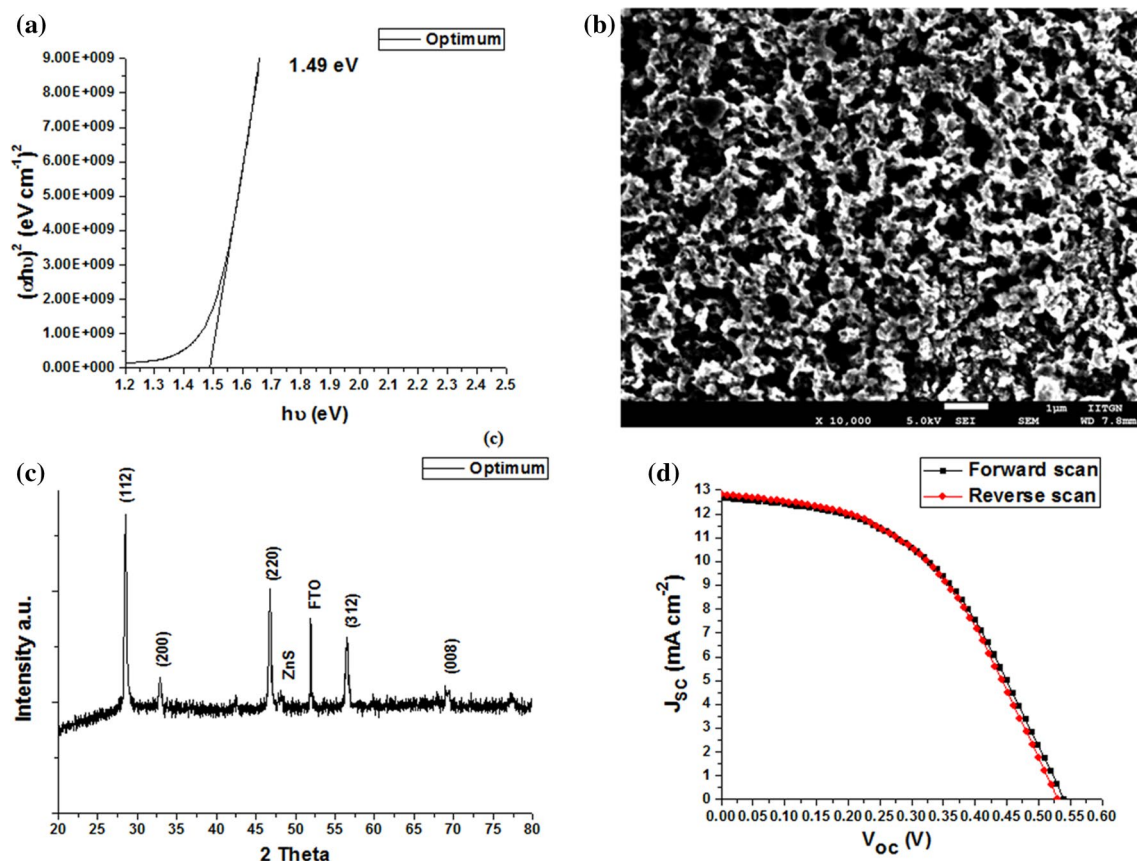


Fig. 6 **a** Band gap of thin film, **b** XRD analysis of the film, **c** surface morphology of the film, **d** J–V characteristics of forward and reverse scan of the solar cell prepared using optimum combination

and $D = 10.97$ s (≈ 11 s) (spray time). The results are in agreement with the results obtained by Taguchi approach. ($A = 0.8$, $B = 1.1$, $C = 320$ °C and $D = 10$ s). Additionally, using ‘Point prediction’ feature of the software also, the optimum result is predicted. The predicted optimum solar cell efficiency is 3.69% with 1.51 eV band gap. The results are also in line with Taguchi results ($3.63 \pm 0.10\%$ and 1.49 eV) as well.

Hence, it can be said clearly that the results of RSM and Taguchi approach are quite similar. Furthermore, a confirmation test is also carried out on the optimum condition obtained with RSM method. A motivating result is obtained with maximum efficiency achievement of 3.65%. Hence, more than 17.7% improvement in efficiency is observed with RSM.

4 Conclusion

In the present study, the effect of four main process parameters, namely, Cu/Zn + Sn ratio, Zn/Sn ratio, substrate temperature and spray time on the properties of spray coated CZTS thin film are studied in detail. For optimization of the process condition, the Taguchi orthogonal (L9) array is applied. The optical analysis suggests that low temperature is attributing more enlargements in band gap due to the presence of secondary phase, confirmed by XRD analysis. Upon increasing the temperature, the band gap closes down to commonly reported band gap (1.4–1.6 eV). However, all the thin film exhibited polycrystalline nature with a preferred orientation of (112) plane, which suggests presence of kesterite structure. Additionally, the prepared thin films are applied in solar cell fabrication. A novel cell fabrication (inverted) FTO/*i*-ZnO/Al:ZnO/CdS/CZTS/CuS/FTO is implemented. The least band gap (1.53 eV) and maximum

Table 7 Box–Behnken design and responses for the band gap and efficiency

Std order	Run order	Process parameters				Responses	
		Cu/Zn+Sn	Zn/Sn	Sub Temp.	Spray Time	Band gap (eV)	Efficiency (%)
1	12	0.8	0.9	320	10	1.60	3.03
2	27	1.2	0.9	320	10	1.71	2.18
3	23	0.8	1.1	320	10	1.52	3.63
4	11	1.2	1.1	320	10	1.60	2.78
5	2	1	1	280	5	1.90	1.43
6	21	1	1	360	5	1.76	1.93
7	7	1	1	280	15	1.88	1.68
8	5	1	1	360	15	1.75	2.18
9	10	0.8	1	320	5	1.61	2.68
10	4	1.2	1	320	5	1.69	1.93
11	26	0.8	1	320	15	1.58	3.08
12	20	1.2	1	320	15	1.66	2.23
13	3	1	0.9	280	10	1.93	1.73
14	15	1	1.1	280	10	1.81	2.38
15	16	1	0.9	360	10	1.79	2.23
16	17	1	1.1	360	10	1.67	2.83
17	24	0.8	1	280	10	1.80	2.43
18	29	1.2	1	280	10	1.88	1.58
19	28	0.8	1	360	10	1.67	2.94
20	1	1.2	1	360	10	1.74	2.08
21	13	1	0.9	320	5	1.73	2.03
22	8	1	1.1	320	5	1.62	2.63
23	6	1	0.9	320	15	1.70	2.33
24	14	1	1.1	320	15	1.59	2.98
25	19	1	1	320	10	1.61	2.98
26	9	1	1	320	10	1.60	2.93
27	18	1	1	320	10	1.61	2.93
28	22	1	1	320	10	1.59	2.93
29	25	1	1	320	10	1.61	2.96

efficiency ($3.10 \pm 0.18\%$) is achieved by R2. The optimum combination ($A_1B_3C_2D_2$; $A=0.8$, $B=1.1$, $C=320$ °C and $D=10$ s) is determined using signal to noise ratio analysis. The contribution of the various control parameters on the result is analyzed by analysis of variance. The substrate temperature is observed to be the most prominent control parameter affecting band gap. Subsequently, Zn/Sn ratio and Cu/Zn + Sn ratio are observed to be second and third most affecting control parameters, respectively. However, spray time is not highly affecting control parameter for the band gap. The confirmation test is also carried out to validate the optimum condition. The film prepared using optimum process condition has outperformed the results achieved by

R2 (1.49 eV). Similarly, efficiency is also improved, variation is decreased and negligible hysteresis effect is achieved ($3.63 \pm 0.10\%$ in forward scan and 3.56 ± 0.14 in reverse scan) by optimization. More than 17% improvement in efficiency is observed. In addition, the RSM is implemented to obtain specific optimum condition from the entire range of parameter. According to RSM, the optimum condition is Cu/Zn + Sn = 0.8, Zn/Sn = 1.1, substrate temperature = 330 °C and spray time = 11 s. A confirmation test is carried out for RSM as well. 3.65% of PCE is achieved using optimum condition obtained by RSM (with 17.7% improvement). Overall, optimum conditions observed can be utilized for further films preparation for solar cells application.

Table 8 ANOVA results of RSM

Source	df	Sum of squares		Means squares		p-value	
		Band Gap	Efficiency	Band gap	Efficiency	Band Gap	Efficiency
Model	14	0.34000	8.03000	0.02400	0.57000	<0.0001	<0.0001
A-Cu/Zn + Sn	1	0.02100	2.08000	0.02100	2.08000	<0.0001	<0.0001
B-Zn/Sn	1	0.03500	1.16000	0.03500	1.16000	<0.0001	<0.0001
C-Sub temp	1	0.05600	0.72000	0.05600	0.72000	<0.0001	<0.0001
D-Spray time	1	0.00188	0.29000	0.00188	0.29000	0.0002	<0.0001
AB	1	0.00023	0.00000	0.00023	0.00000	0.1045	1
AC	1	0.00003	0.00003	0.00003	0.00003	0.572	0.9056
AD	1	0.00000	0.00160	0.00000	0.00160	1	0.3506
BC	1	0.00000	0.00010	0.00000	0.00010	1	0.8127
BD	1	0.00000	0.00063	0.00000	0.00063	1	0.5558
CD	1	0.00003	0.00000	0.00003	0.00000	0.572	1
A ²	1	0.00075	0.00000	0.00075	0.00000	0.0068	0.996
B ²	1	0.00156	0.00201	0.00156	0.00201	0.0004	0.2979
C ²	1	0.21000	2.74000	0.21000	2.74000	<0.0001	<0.0001
D ²	1	0.01100	1.21000	0.01100	1.21000	<0.0001	<0.0001
Residual	14	0.00105	0.02400	0.00007	0.00172		
Lack of fit	10	0.00073	0.01500	0.00007	0.00147	0.5932	0.7476
Pure error	4	0.00032	0.00932	0.00008	0.00233		
Total	28	0.34000	8.05000				

df degree of freedom

*Significant $p < 0.05$

References

- N. Ali, A. Hussain, R. Ahmed, M.K. Wang, C. Zhao, B.U. Haq, Y.Q. Fu, *Renew. Sustain. Energy Rev.* **59**, 726 (2016)
- X. Zeng, K.F. Tai, T. Zhang, C.W.J. Ho, X. Chen, A. Huan, T.C. Sum, L.H. Wong, *Sol. Energy Mater. Sol. Cells* **124**, 55 (2014)
- R. Liu, M. Tan, X. Zhang, J. Chen, S. Song, W. Zhang, *J. Alloys Compd.* **655**, 124 (2016)
- Z. Shi, D. Attygalle, A.H. Jayatissa, *J. Mater. Sci. Mater. Electron.* **28**, 2290 (2017)
- I.G. Orletskyi, M.M. Solovan, V.V. Brus, F. Pinna, G. Cicero, P.D. Maryanchuk, E.V. Maistruk, M.I. Ilashchuk, T.I. Boichuk, E. Tresso, *J. Phys. Chem. Solids* **100**, 154 (2017)
- M.A. Green, K. Emery, Y. Hishikawa, W. Warta, E.D. Dunlop, D.H. Levi, A.W.Y. Ho-Baillie, *Prog. Photovolt. Res. Appl.* **25**, 3 (2017)
- W. Shockley, H.J. Queisser, *J. Appl. Phys.* **32**, 510 (1961)
- Y.P. Lin, Y.F. Chi, T.E. Hsieh, Y.C. Chen, K.P. Huang, *J. Alloys Compd.* **654**, 498 (2016)
- E.M. Mkawi, K. Ibrahim, M.K.M. Ali, K.M.A. Saron, M.A. Farukh, N.K. Allam, *J. Mater. Sci. Mater. Electron.* **26**, 222 (2014)
- E. Garcia-Llamas, J.M. Merino, R. Gunder, K. Neldner, D. Greiner, A. Steigert, S. Giraldo, V. Izquierdo-Roca, E. Saucedo, M. León, S. Schorr, R. Caballero, *Sol. Energy* **141**, 236 (2017)
- A. Cazzaniga, A. Crovetto, C. Yan, K. Sun, X. Hao, J. RamisEstelrich, S. Canulescu, E. Stamate, N. Pryds, O. Hansen, J. Schou, *Sol. Energy Mater. Sol. Cells* **166**, 91 (2017)
- T. Washio, T. Shinji, S. Tajima, T. Fukano, T. Motohiro, K. Jimbo, H. Katagiri, *J. Mater. Chem.* **22**, 4021 (2012)
- S.B. Patel, J.V. Gohel, *Phys. Astron. Int. J.* **1**, 1 (2017)
- M. Courel, J.A. Andrade-Arvizu, A. Guillén-Cervantes, M.M. Nicolás-Marín, F.A. Pulgarín-Agudelo, O. Vigil-Galán, *Mater. Des.* **114**, 515 (2017)
- P.S. Mishra, J.N. Solanki, Z.V.P. Murthy, *Cryst. Res. Technol.* **48**, 969 (2013)
- M.T. Winkler, W. Wang, O. Gunawan, H.J. Hovel, T.K. Todorov, D.B. Mitzi, *Energy Environ. Sci.* **7**, 1029 (2014)
- M. Boshta, S. Binetti, A. Le Donne, M. Gomaa, M. Acciarri, *Mater. Technol.* **32**, 251 (2017)
- V.G. Rajeshmon, C.S. Kartha, K.P. Vijayakumar, C. Sanjeeviraja, T. Abe, Y. Kashiwaba, *Sol. Energy* **85**, 249 (2011)
- S. Das, C. Frye, P.G. Muzykov, K.C. Mandal, *ECS Trans.* **45**, 153 (2012)
- M.A. Majeed Khan, S. Kumar, M. Alhoshan, A.S. Al Dwayyan, *Opt. Laser Technol.* **49**, 196 (2013)
- R.J. Deokate, A.D. Adsool, N.S. Shinde, S.M. Pawar, C.D. Lokhande, *Energy Procedia* **54**, 627 (2014)
- S.K. Swami, N. Chaturvedi, A. Kumar, V. Dutta, *Sol. Energy* **122**, 508 (2015)
- M. Espindola-Rodriguez, Y. Sanchez, S. Lopez-Marino, D. Sylla, M. Placidi, M. Neuschitzer, H. Xie, V. Izquierdo-Roca, O. Vigil-Galan, E. Saucedo, *J. Anal. Appl. Pyrolysis* **120**, 45 (2016)
- O. Vigil-Galan, M. Espindola-Rodriguez, M. Courel, X. Fontane, D. Sylla, V. Izquierdo-Roca, A. Fairbrother, E. Saucedo, A. Perez-Rodriguez, *Sol. Energy Mater. Sol. Cells* **117**, 246 (2013)
- S.B. Patel, J.V. Gohel, in *Recent Advances in Photocatalytic Nanomaterials for Environmental Applications* (Materials Research Forum LLC, Millersville, PA, 2018), pp. 367–400
- S.M. Bhosale, M.P. Suryawanshi, M.A. Gaikwad, P.N. Bhosale, J.H. Kim, A.V. Moholkar, *Mater. Lett.* **129**, 153 (2014)
- M. Valdes, G. Santoro, M. Vazquez, *J. Alloys Compd.* **585**, 776 (2014)
- O. Vigil-Galán, M. Courel, M. Espindola-Rodriguez, D. Jiménez-Olarte, M. Aguilar-Frutis, E. Saucedo, *Sol. Energy Mater. Sol. Cells* **132**, 557 (2015)

29. S.M. Bhosale, M.P. Suryawanshi, J.H. Kim, A.V. Moholkar, *Ceram. Int.* **41**, 8299 (2015)
30. S. Kermadi, S. Sali, F. AitAmeur, L. Zougar, M. Boumaour, A. Toumiat, N.N. Melnik, D.W. Hewak, A. Duta, *Mater. Chem. Phys.* **169**, 96 (2016)
31. M. Courel, E. Valencia-Resendiz, J.A. Andrade-Arvizu, E. Saucedo, O. Vigil-Galán, *Sol. Energy Mater. Sol. Cells* **159**, 151 (2017)
32. M. Espindola-Rodriguez, M. Placidi, O. Vigil-Galan, V. Izquierdo-Roca, X. Fontane, A. Fairbrother, D. Sylla, E. Saucedo, A. Perez-Rodriguez, *Thin Solid Films* **535**, 67 (2013)
33. J. Chen, Q. Chen, Y. Ni, Y. Yamaguchi, T. Wang, Z. Jia, X. Dou, S. Zhuang, *J. Sol-Gel Sci. Technol.* **75**, 25 (2015)
34. V.G. Rajeshmon, M.R.R. Menon, C.S. Kartha, K.P. Vijayakumar, *J. Anal. Appl. Pyrolysis* **110**, 448 (2014)
35. S.A. Weissman, N.G. Anderson, *Org. Process Res. Dev.* **19**, 1605 (2015)
36. E. Yucel, Y. Yucel, M. Durak, *J. Mater. Sci. Mater. Electron.* **28**, 2206 (2017)
37. X.L. Wei, Y. Xia, X.M. Liu, H. Yang, X.D. Shen, *Electrochim. Acta* **136**, 250 (2014)
38. G.E.P. Box, N.R. Draper, *Wiley Series in Probability and Mathematical Statistics* (Wiley, New York, 1987), p. 669
39. J.C. Venter, H.O. Smith, L. Hood, *Nature* **381**, 364 (1996)
40. N. Kumari, J.V. Gohel, S.R. Patel, *Opt. Int. J. Light Electron. Opt.* **144**, 422 (2017)
41. M. Lanjewar, J.V. Gohel, *Inorg. Nano-Metal Chem.* **47**, 1090 (2017)
42. J.V. Gohel, A.K. Jana, M. Singh, *Appl. Phys. A* **123**, 1 (2017)
43. X. Yan, X. Hu, S. Komarneni, *J. Korean Phys. Soc.* **66**, 1511 (2015)
44. K. Ramasamy, M.A. Malik, P. O'Brien, *Chem. Sci.* **2**, 1170 (2011)
45. W. Wang, H. Shen, X. He, J. Li, *J. Nanoparticle Res.* **16**, (2014)
46. D. Pareek, K.R. Balasubramaniam, P. Sharma, *Mater. Charact.* **103**, 42 (2015)
47. K. Mokurla, S. Mallick, P. Bhargava, *Energy Procedia* **57**, 73 (2014)
48. N. Kamoun, H. Bouzouita, B. Rezig, *Thin Solid Films* **515**, 5949 (2007)
49. Y.B. Kishore Kumar, G. Suresh Babu, P. UdayBhaskar, V. Sundara Raja, *Sol. Energy Mater. Sol. Cells* **93**, 1230 (2009)
50. S. Thiruvenkadam, D. Jovina, A. Leo Rajesh, *Sol. Energy* **106**, 166 (2014)
51. A. Chavda, M. Patel, I. Mukhopadhyay, A. Ray, *ACS Sustain. Chem. Eng* **4**, 2302 (2016)
52. W. Daranf, M.S. Aida, N. Attaf, J. Bougdira, H. Rinnert, *J. Alloys Compd.* **542**, 22 (2012)
53. G. Chen, C. Yuan, J. Liu, Z. Huang, S. Chen, W. Liu, G. Jiang, C. Zhu, *J. Power Sources* **276**, 145 (2015)
54. J. Cheng, Z. Dai, B. Chen, R. Ji, X. Yang, R. Hu, J. Zhu, L. Li, *Nanoscale Res. Lett.* **11**, 550 (2016)
55. S.C. Riha, B.A. Parkinson, A.L. Prieto, *J. Am. Chem. Soc.* **131**, 12054 (2009)
56. Q. Guo, H.W. Hillhouse, R. Agrawal, *J. Am. Chem. Soc.* **131**, 11672 (2009)
57. S. Chen, H. Tao, Y. Shen, L. Zhu, X. Zeng, J. Tao, T. Wang, *RSC Adv.* **5**, 6682 (2015)
58. W. Xiao, J.N. Wang, X.S. Zhao, J.W. Wang, G.J. Huang, L. Cheng, L.J. Jiang, L.G. Wang, *Sol. Energy* **116**, 125 (2015)